Nonpolarized Cells Selectively Sort Apical Proteins from Cell Surface to a Novel Compartment, but Lack Apical Retention Mechanisms

Pamela L. Tuma, Lydia K. Nyasae, and Ann L. Hubbard*

Department of Cell Biology, Johns Hopkins University School of Medicine, Baltimore, Maryland 21205

Membrane trafficking is central to establishing and maintaining epithelial cell polarity. One open question is to what extent the mechanisms regulating membrane trafficking are conserved between nonpolarized and polarized cells. To answer this question, we examined the dynamics of domain-specific plasma membrane (PM) proteins in three classes of hepatic cells: polarized and differentiated WIF-B cells, nonpolarized and differentiated Fao cells, and nonpolarized and nondifferentiated Clone 9 cells. In nonpolarized cells, mature apical proteins were uniformly distributed in the PM. Surprisingly, they were also in an intracellular compartment. Double labeling revealed that the compartment contained only apical proteins. By monitoring the dynamics of antibody-labeled molecules in nonpolarized cells, we further found that apical proteins rapidly recycled between the compartment and PM. In contrast, the apical PM residents in polarized cells showed neither internalization nor return to the basolateral PM from which they had originally come. Cytochalasin D treatment of these polarized cells revealed that the retention mechanisms are actin dependent. We conclude from these data that both polarized and nonpolarized cells selectively sort apical proteins from the PM and transport them to specific, but different cellular locations. We propose that the intracellular recycling compartment in nonpolarized cells is an intermediate in apical surface formation.

INTRODUCTION

The major epithelial cell of the liver, the hepatocyte, is characterized by multiple levels of structural asymmetry that are reflected in cell shape, cytoskeletal and organelle distribution, and cell surface composition. The hepatocyte plasma membrane (PM) is divided into two distinct domains: the apical surface (that faces the bile) and the basolateral, which includes the lateral surface (that faces adjacent cells) and the basal surface (that faces the blood in the spaces of Disse) (reviewed in Tuma and Hubbard, 2001). Each domain performs specific activities that rely on the presence of distinct sets of proteins and lipids. Although the establishment and maintenance of hepatocyte polarity are imperative for proper liver function, little is known about the mechanisms that regulate these processes. From studies performed in fetal liver, we found that cell surface differentiation occurs early and that the PM is already polarized by the time the liver and resident hepatocytes can be identified (Feracci *et al.*, 1987). Furthermore, in regenerating liver, dividing hepatocytes maintain their PM polarity (Bartles and Hubbard, 1986). These experimental limitations have prevented us from observing the initial steps in the development of PM polarity in vivo so we turned to nonpolarized and polarized cells in vitro.

The mechanisms regulating the delivery of proteins and lipids to the PM in polarized epithelial cells have been explored extensively. Because polarized cells have two distinct PM domains, an early view was that the mechanisms in polarized cells must be more complex than those in nonpolarized cells. Multiple sets of vesicles and associated machinery were hypothesized to exist that specifically delivered cargo to each domain. Consistent with this idea, distinct

apical-targeted vesicles were identified (Wandinger-Ness *et al.*, 1990) as well as epithelial-specific, apical-targeting molecules such as annexin XIIIb and the GTPase rab17 (Lutcke *et al.*, 1993; Fiedler *et al.*, 1995).

Recent studies in nonpolarized cells suggest that all cells are equipped for polarized protein delivery. From work in virally infected, nonpolarized 3T3, baby hamster kidney, and Chinese hamster ovary cells, distinct *trans*-Golgi network (TGN)-derived vesicles were identified that contained cargo that would be delivered specifically to either the apical or basolateral PM in polarized cells (Musch *et al.*, 1996; Yoshimori *et al.*, 1996). Delivery of these vesicles to the PM was also differentially regulated by G proteins and soluble *N*-ethylmaleimide-sensitive factor attachment protein receptors in nonpolarized cells as they were in polarized Madin-Darby canine kidney (MDCK) cells (Yoshimori *et al.*, 1996). These results suggest that nonpolarized cells have the requisite machinery, and thus capacity, for polarized PM delivery, but merely lack the spatial segregation of distinct membrane targets.

Delivery is only part of the life cycle of PM proteins. What happens to domain-specific proteins once they have reached the cell surface? Are they retained? Do they recycle or are they degraded? What happens in nonpolarized hepatic cells? In polarized hepatocytes, the predominant pathway that newly synthesized apical proteins take to the apical PM is indirect (Bartles *et al.*, 1987; Bartles and Hubbard 1988; Schell *et al.*, 1992). They are transported from the TGN to the basolateral PM where they are selectively internalized and transcytosed to the apical surface. If nonpolarized hepatic cells are equipped for polarized PM transport beyond the delivery step, the indirect pathway must also be part of their vesicle-trafficking repertoire.

We examined the itineraries of resident apical and basolateral PM proteins in three classes of hepatic cells: polarized and differentiated WIF-B cells; nonpolarized, yet differentiated Fao cells; and nonpolarized, nondifferentiated Clone 9 cells. Although Clone 9 cells were derived from normal rat liver and retain an epithelial morphology, they do not polarize and no longer express liver-specific activities (Weinstein *et al.*, 1975). We found that the two classes of nonpolarized cells discriminate between domain-specific proteins at the PM and transport only "would-be" apical proteins to a novel compartment. However, these apical proteins recycle between the compartment and PM in nonpolarized cells, unlike their counterparts in fully polarized WIF-B cells where actin-dependent mechanisms normally prevent return. Thus, nonpolarized cells are capable of polarized membrane sorting and transport, but lack apical-specific retention mechanisms.

MATERIALS AND METHODS

Reagents and Antibodies

Nocodazole, horseradish peroxidase (HRP) (type VI), and cytochalasin D (CD) were purchased from Sigma-Aldrich (St. Louis, MO) and were stored as stock solutions at −20°C. Fluorescein isothiocyanate (FITC)-conjugated dextrans (molecular weight 4.4 or 71.2 kDa) were also purchased from Sigma-Aldrich. Culture media and fetal bovine serum (FBS) were purchased from Invitrogen (Carlsbad, CA). Alexa 488 and 568-conjugated secondary antibodies and Texas Red-phalloidin were from Molecular Probes (Eugene, OR). Anti-β-tubulin, anti-transferrin receptor (Tf-R; monoclonal anti-

body), and anti-rab11a antibodies were purchased from Sigma-Aldrich, Accurate Chemical & Scientific (Westbury, NY), and Zymed Laboratories (South San Francisco, CA), respectively. Anti-E-cadherin, anti-β-catenin, and anti-early endosomal antigen 1 (EEA1) antibodies were all purchased from Transduction Laboratories (Lexington, KY). The antibodies against Tf-R (polyclonal), multidrug resistance-associated protein 2 (MRP2), mannose 6-phosphate receptor (M6P-R), rab5, rab3D, 5′-nucleotidase (5′NT), lysosomal glycoprotein 120, and ezrin binding protein 50 (EBP50) were kindly provided by M. Farquhar (University of California, San Diego, CA), D. Keppler (Deutsches Krebsforschungszentrum, Heidelberg, Germany), P. Nissley (National Institutes of Health, Bethesda, MD), G. Quellhorst and M. Wessling-Resnick (Harvard School of Public Health, Boston, MA), J. Larkin (Barnard College, New York, NY), J.P. Luzio (Cambridge University, Cambridge, United Kingdom), W. Dunn (University of Florida, Gainesville, FL), and C. Chen (Johns Hopkins University School of Medicine, Baltimore, MD), respectively. Ezrin and radixin antibodies were kindly provided by M. Arpin (Curie Institute, Paris, France). Antibodies against aminopeptidase N (APN) asialoglycoprotein receptor (ASGP-R), CE9, HA321, dipeptidylpeptidase IV (DPP IV), polymeric IgA-receptor (pIgA-R), and endolyn-78 were prepared by the Hubbard laboratory and have been described previously (Hubbard *et al.*, 1985; Scott and Hubbard, 1992; Barr and Hubbard, 1993; Ihrke *et al.*, 1993, 1998; Shanks *et al.*, 1994).

Cell Culture

WIF-B and Fao cells were grown in a humidified 7% CO_2 incubator at 37°C as described previously (Ihrke *et al.*, 1993; Shanks *et al.*, 1994). Briefly, cells were grown in F-12 medium (Cassio modification), pH 7.0, supplemented with 5% FBS. WIF-B medium was also supplemented with 10 μM hypoxanthine, 40 nM aminoterpin, and 1.6 μM thymidine. Clone 9 cells were grown in Ham's F-12 media supplemented with 10% FBS in a 5% CO_2 incubator at 37°C. For immunostaining and quantitative assays, cells were seeded onto glass coverslips at 1.3×10^4 cells/cm². Fao and Clone 9 cells were cultured for 3–5 d and WIF-B cells for 8–12 d until they reached maximum density and polarity.

Exogenous Expression of DPP IV

Clone 9 cells were infected with recombinant adenovirus particles (0.7–1.4×10^{10} virus particles/ml) encoding full-length DPP IV for 30 min at 37°C as described previously (Bastaki *et al.*, 2002). The cells were washed with complete medium and incubated an additional 24 h. To inhibit protein synthesis and rid the biosynthetic pathway of DPP IV, cells were treated with 100 μg/ml cycloheximide for 3 h in serum-free medium before immunolabeling.

Immunofluorescence Microscopy

In general, cells were fixed on ice with chilled phosphate-buffered saline (PBS) containing 4% paraformaldehyde (PFA) for 1 min and permeabilized with ice-cold methanol for 10 min. To detect MRP2, cells were fixed and permeabilized at −20°C with methanol for 5 min. To detect ezrin and EBP50, cells were permeabilized for 5 min at room temperature (RT) with 0.1% saponin prepared in PEM (100 mM PIPES, 1 mM EGTA, 1 mM $MgSO_4$, pH 6.8) containing 8% sucrose and fixed in 4% PFA/PBS for 30 min at RT. To detect rab11a, cells were fixed at RT for 15 min with 4% PFA/PBS (prewarmed to 37°C) and permeabilized for 5 min at RT with 0.1% Triton X-100/PBS. Cells were processed for indirect immunofluorescence as described previously (Ihrke *et al.*, 1998). Rabbit polyclonal antibodies against ASGP-R, M6P-R, pIgA-R, and rab11a were diluted 1:100. MRP2, LGP-120, Tf-R, DPP IV, APN, ezrin, and radixin polyclonal antibodies were used at 1:200. Polyclonal anti-EBP50 and anti-rab3D were diluted 1:1000. Anti-5′NT, anti-endolyn-78, and anti-EEA1 mouse monoclonal antibody were diluted 1:300, 1:500, and 1:40,

respectively. Purified IgG fraction of anti-HA321 from mouse ascites was diluted 1:500. Alexa 488- or 568-conjugated secondary antibodies were used at 3–5 μg/ml.

To depolymerize microtubules (MTs), 33 μM nocodazole was used (Figure 8). Staining with anti-β-tubulin antibodies (1:500) was used to assess the extent of MT disruption. To disrupt actin filaments, Fao and WIF-B cells were treated with 1 or 10 μM CD, respectively (Figure 9). Texas Red-phalloidin (50 U/ml) staining was used to assess the extent of actin disruption. For optimal staining with phalloidin, cells were fixed for 5 min at −20°C with prechilled methanol.

To assess tight junction integrity after CD treatment, the permeability properties of WIF-B bile canaliculi (BCs) were tested with differently sized FITC-conjugated dextrans as described previously (Ihrke *et al.*, 1993). Briefly, the dextrans (4.4 or 71.2 kDa) were diluted in prewarmed complete medium to a final concentration of 10 mg/ml. WIF-B cells treated in the absence or presence of 10 μM CD for 1 h were rinsed briefly in prewarmed medium and incubated an additional 10 min with the dextrans at 37°C. After rinsing 2–3 times with prewarmed medium, the dextrans in live cells were immediately visualized on a Axioplan fluorescence microscope (Carl Zeiss, Jena, Germany) by using a 40× objective under phase contrast or epifluorescence illumination. Fluorescent BCs were counted on micrographs and expressed as percentage of total BC observed by phase microscopy.

Internalization Assays

Fao cells were incubated on ice for 5 min in HEPES-buffered (20 mM, pH 7.0), serum-free medium (HSFM). Cell surface antigens were labeled at 4°C for 15 min with specific antibodies. Rabbit polyclonals were diluted 1:50 to 1:100 in HSFM containing 2 mg/ml bovine serum albumin, and mouse anti-5′NT (purified IgG) was used at 20 μg/ml. After labeling, cells were washed in HSFM containing 2 mg/ml bovine serum albumin, placed in prewarmed complete medium, and incubated at 37°C for the indicated times. The cells were fixed and permeabilized as described above. The trafficked antibodies were labeled with Alexa 488 or 568-conjugated secondary antibodies (3–5 μg/ml).

In Figure 4B, cells were imaged with an Ultraview confocal. Regions of interest containing the juxtanuclear clusters were selected from 20 (e–g) or 40 (h–j) cells, and overlapping fluorescence signals were measured on a pixel-by-pixel basis by using the Colocalization Analysis Tool of the Ultraview Imaging Software Spatial Module (Ultraview, Orinda, CA). Values from the individual cells were averaged and the SDs calculated. The cells imaged and analyzed in e–g were from two independent experiments, whereas those in h–j were from three independent experiments.

Recycling Assays

Fao Cells. Apical proteins were labeled and chased as described for the internalization assays (see figure legends for details). To strip antibodies from their surface antigens, cells were rinsed briefly with prewarmed PBS and incubated in isoglycine (200 mM glycine, 150 mM NaCl, pH 2.5) for 5 min at RT. The cells were rinsed with PBS, placed in prewarmed complete medium and incubated at 37°C for the desired times. The total population of antibody–antigen complexes was detected with secondary antibodies in cells fixed as described above, whereas the cell surface population was detected in cells fixed with 4% PFA in PBS for 30 min at RT.

WIF-B Cells. Cells were continuously labeled with anti-APN, 5′NT, or pIgA-R antibodies (1:500, 1:1000, and 1:200, respectively) diluted in complete medium for 1 h at 37°C. Because tight junctions restrict antibody access to the apical PM, only apical proteins present at the basolateral PM were labeled. Cells were washed three times for 2 min each with prewarmed medium and incubated an additional hour at 37°C to chase the antibody–antigen complexes to the apical

PM. Because WIF-B cells were more sensitive than Fao cells to prolonged isoglycine incubations, the residual antibodies at the basolateral PM were stripped with isoglycine (400 mM glycine, 150 mM NaCl, pH 2.5) for 2 min at 37°C. The cells were then rinsed with PBS, placed in prewarmed complete medium and incubated at 37°C for the desired times. The total population of antibody–antigen complexes was detected with secondary antibodies in fixed and permeabilized cells as described above.

Kinetic Assays

Total IgG from serum (APN or DPP IV) or hybridoma supernatant (Tf-R) was purified using EZ-Sep (Pharmacia AB, Uppsala, Sweden) and biotinylated using EZ-Link Sulfo-NHS-biotin (Pierce Chemical, Rockford, IL) according to the manufacturers' instructions. To measure internalization, Fao cells were continuously labeled with biotinylated antibodies for the indicated times at 37°C. The remaining cell surface-associated antibodies were eluted with isoglycine as described above, and the cells were lysed in isoglycine containing 20 mM octylglucoside and 0.5% Triton X-100 for 30 min on ice. Aliquots of the eluate and lysate were incubated in streptavidin-coated 96-well plates (Pierce Chemical). Bound antibodies were detected with HRP-conjugated secondary antibodies (Amersham Biosciences, Piscataway, NJ) followed by colorimetric detection with an HRP substrate detection kit (Bio-Rad, Hercules, CA). All points were performed in duplicate. To measure recycling, cells were continuously labeled with biotinylated antibodies for 2 h at 37°C, eluted as described above, and placed in complete medium at 37°C for the indicated times. Cells were eluted again (representing the recycled population) and then lysed as described above. The eluates and lysates were processed as for the internalization assays. Numbers were corrected for the percentage of cells that survived acid stripping as assayed by trypan blue exclusion.

Imaging

Labeled cells were visualized by confocal microscopy (Ultraview) in Figure 4B. All others were visualized by epifluorescence (Axioplan Universal Microscope; Carl Zeiss). Images were acquired with a Princeton MicroMax cooled charge-coupled device camera (Roper Scientific, Trenton, NJ) and IP Labs software (Scanalytics, Fairfax, VA). Further image processing and figure compilation were performed using Photoshop (Adobe Systems, Mountain View, CA) and PowerPoint software (Microsoft, Redmond, WA).

RESULTS

Apical Proteins Are Present at PM and in a Novel Compartment in Nonpolarized Hepatic Cells

We first determined the steady-state locations of domain-specific PM proteins in the three classes of hepatic cells. As we have described previously in polarized WIF-B cells, apical and basolateral PM proteins have complementary distributions. Examples are shown in Figure 1. Like all other resident apical proteins examined, APN expression was restricted to the membrane that lines the large structures representing BC (the apical domains) formed between adjacent cells (Figure 1a). All basolateral residents tested had reciprocal staining patterns. The distribution of HA321 is shown in Figure 1b. Because the single transmembrane domain (TMD) and glycosylphosphatidylinositol (GPI)-anchored apical PM residents that we have examined in WIF-B cells behave similarly with respect to their distributions and dynamics (Ihrke *et al.*, 1993, 1998, Tuma *et al.*, 1999, 2001), we have used them interchangeably in this study.

Unlike for polarized cells, apical and basolateral proteins showed overlapping expression at the PM in nonpolarized Fao (Figure 1, c and d) and Clone 9 cells (Figure 1, e and f).
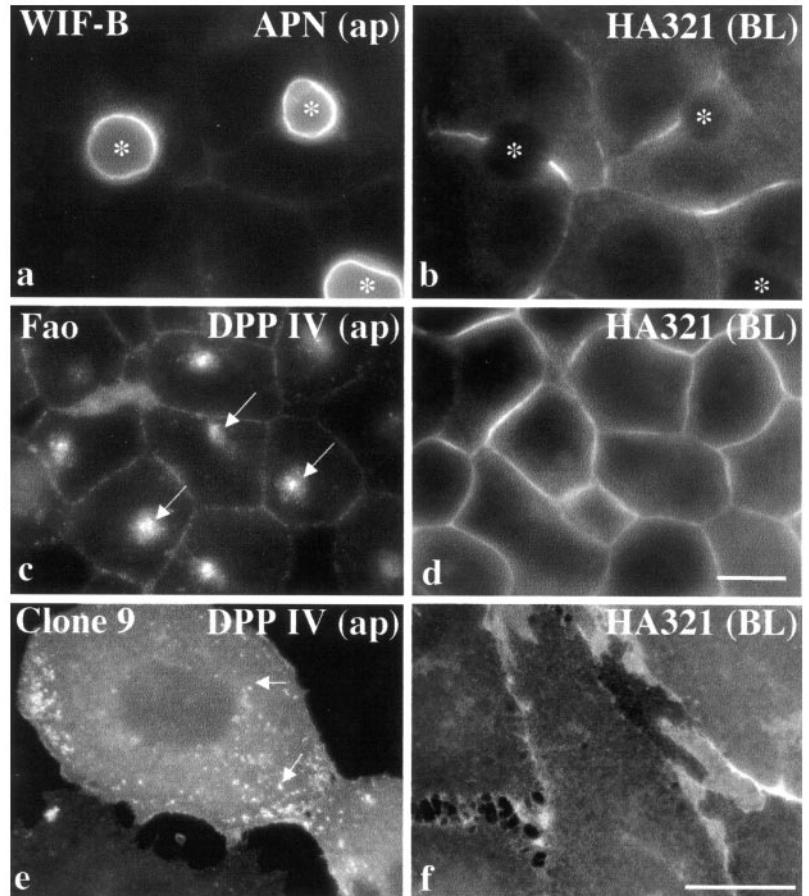
Figure 1. Apical proteins are present at the PM and in an intracellular compartment in nonpolarized hepatic cells. Three classes of hepatic cells were immunolabeled for resident apical and basolateral proteins. Staining of polarized and differentiated WIF-B cells (a and b); of nonpolarized, differentiated Fao cells (c and d); and nonpolarized, nondifferentiated Clone 9 cells (e and f) is shown. The proteins were endogenously expressed except for DPP IV in Clone 9 cells, which was introduced with recombinant adenovirus. To deplete newly synthesized DPP IV from the biosynthetic pathway, Clone 9 cells were incubated for 3 h with 100 μg/ml cycloheximide. Arrows in c and e point to intracellular structures containing apical proteins in nonpolarized cells. Ap, apical; BL, basolateral. Bar, 10 μm.

However, the apical proteins were also observed in small puncta either in a juxtanuclear compartment (Fao; Figure 1c) or dispersed (Clone 9; Figure 1e). In Figure 2, the distributions of multiple basolateral and apical PM proteins in Fao cells are shown. As observed for HA321, all of the basolateral residents we examined were present only at the PM. No intracellular populations of CE9 or E-cadherin or (Figure 2, a and b, respectively) were observed. β-Catenin, a peripherally associated basolateral protein, was also predominantly expressed at the PM in Fao cells (Figure 2c). A small intracellular pool was observed that did not colocalize with the apical PM proteins (our unpublished data). Conversely, all classes of apical PM residents we examined were present both at the PM and in an intracellular pool. As shown in Figure 2, d–f, the single TMD protein APN nearly perfectly colocalized with the GPI-anchored apical protein 5'NT. Likewise, the single TMD protein DPP IV and the polytopic apical resident MRP2 were present both at the PM and in the same intracellular compartment (Figure 2, g–i). The transcytosing receptor pIgA-R was also present in the compartment (our unpublished data). Different combinations of the apical proteins all showed overlapping staining patterns (our unpublished data), thus the apical markers in nonpolarized cells were also used interchangeably throughout the study. Finally, rab3D, a GTPase peripherally associated with the

hepatic apical PM (Larkin *et al.*, 2000), was also present in the intracellular compartment (Figure 2, j–l).

We next asked whether the compartment was a biosynthetic organelle (Figure 2, m–o). Although DPP IV and TGN38 were both detected in juxtanuclear structures, the merged images revealed that the staining patterns did not overlap. Similarly, 5'NT positive structures did not label for albumin, a major hepatic secretory protein that is present in high amounts in the endoplasmic reticulum and Golgi (our unpublished data). Moreover, treatment of Fao cells with 25 μg/ml cycloheximide to inhibit protein synthesis did not alter the intracellular apical protein staining pattern, indicating that the compartment was not a biosynthetic organelle (our unpublished data).

To determine whether the compartment was a lysosome, Fao cells were double labeled for APN and endolyn-78 (a lysosomal membrane protein). Although both markers were present in the same region of the cell, they did not overlap, indicating that APN was not in lysosomes (Figure 3, a–c). Similar results were observed when cells were stained for 5'NT and another lysosomal protein, LGP-120 (our unpublished data). To determine whether the intracellular structures were a known endosomal compartment, we double labeled Fao cells for apical proteins and different endosome markers. Early endosomes were labeled with ASGP-R, late
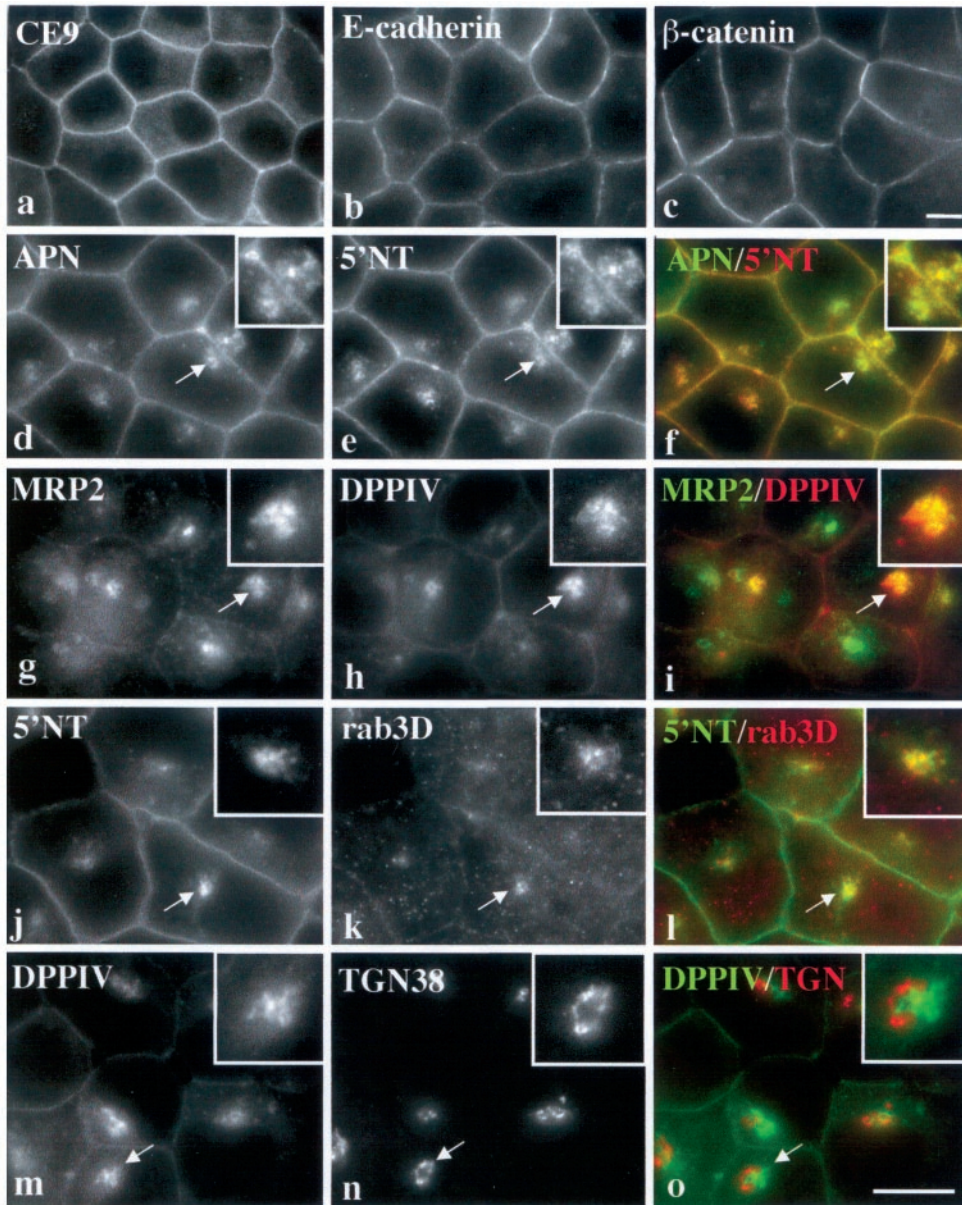
Figure 2. The intracellular compartment contains apical, but not basolateral resident proteins. Fao cells were stained for the basolateral resident proteins CE9 (a), E-cadherin (b), and β-catenin (c). No intracellular staining for these markers was observed. Fao cells were also double labeled for different combinations of apical resident proteins. APN colabeled with 5'NT (d–f), MRP2 with DPP IV (g–i), and 5'NT with rab3D (j–l) are shown. In all cases, substantial colocalization was observed at the intracellular compartment. DPP IV and TGN38 double labeling is also shown (m–o). Merged images are shown (f, i, l, and o). Arrows are pointing to the intracellular clusters enlarged in the insets approximately twofold. Bar, 10 μm.

endosomes were labeled with M6P-R, and recycling endosomes were labeled with Tf-R or rab11a. As shown in Figure 3, d–o, none of the endosome staining patterns significantly overlapped with that of 5'NT or APN. Only Tf-R staining was seen to minimally overlap (Figure 4; see below). Additionally, rab5 and EEA1 (other early endosome markers) were not present in the apical structures (our unpublished data). Furthermore, immunolabeled HRP that was continuously administered for 1 h did not overlap with 5'NT (our unpublished data). These results indicate that the compartment is not a known endosome.

The Compartment Is Dynamic and Selective

To determine whether the compartment received apical proteins internalized from the cell surface, we antibody labeled

apical proteins present at the PM at 4°C. The cells were warmed to 37°C and the antibody–antigen complexes chased for the indicated times. PM labeling of APN at 4°C was observed with no corresponding intracellular staining (Figure 4a). After warm-up, the apical proteins were observed in intracellular structures in Fao (Figure 4b) and Clone 9 (Figure 4c) cells. We also monitored the dynamics of the antibody-labeled basolateral protein HA321 in nonpolarized cells. As for APN, PM labeling was observed at 4°C (our unpublished data). However, after warm-up, no intracellular populations of HA321 were detected (Figure 4d).

To determine whether the structures that received apical proteins internalized from the cell surface were the same as those containing apical proteins at steady state, we colabeled Fao cells for trafficked APN–antibody complexes and 5'NT
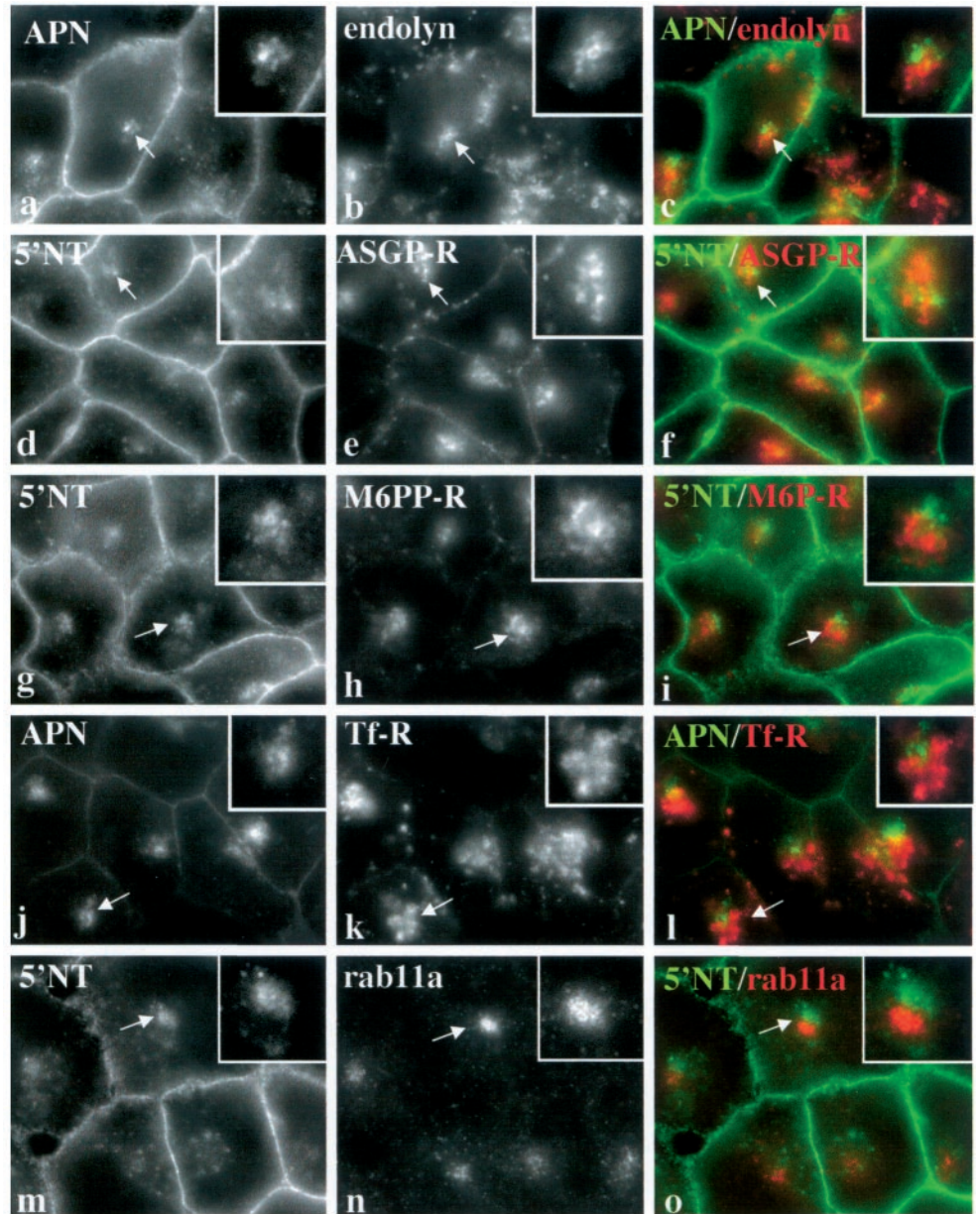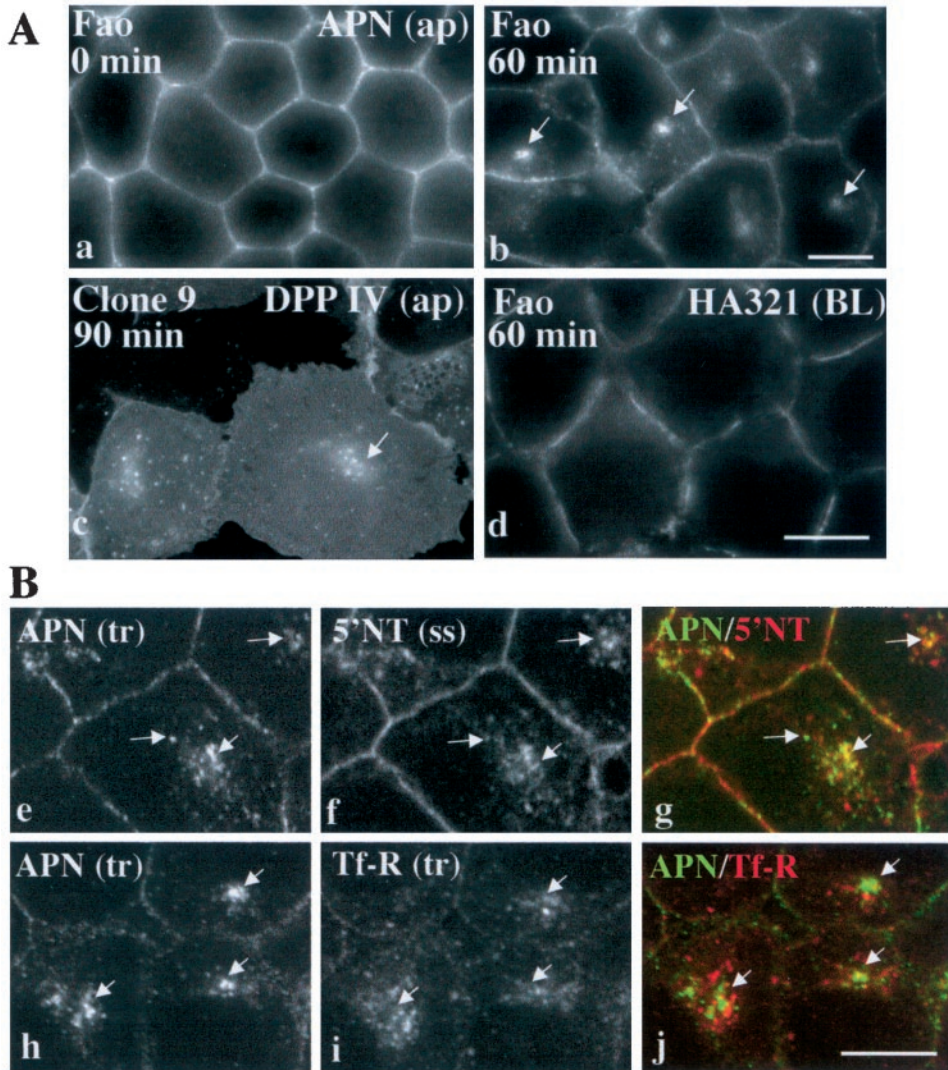
Figure 3. The intracellular compartment is novel. Fao cells were double labeled for APN and endolyn-78 (a–c), 5'NT and ASGP-R (d–f), 5'NT and M6P-R (g–i), APN and Tf-R (j–l), or 5'NT and rab11a. Merged images are shown (c, f, i, l, and o). Arrows are pointing to the intracellular clusters enlarged in the insets approximately twofold. Bar, 10 μm.

steady-state distributions. Although internalized APN staining was not as bright as 5'NT steady-state staining, the patterns overlapped (compare Figure 4, e and f). From confocal images we determined that the extent of overlap of the two fluorescence signals was nearly 70% (67.3 ± 17.5%). In contrast, when APN and Tf-R trafficking was monitored simultaneously, the staining patterns minimally overlapped (Figure 4, g and h). Less than 15% (14.7 ± 19.1%) of APN and Tf-R was present in the same structures. The trafficked antibodies in these experiments were continuously administered such that the overlapping signals may indicate the presence of a common transport intermediate (early endosome?). Together, these results indicate that nonpolarized hepatic cells discriminate among apical proteins, basolateral

proteins, and recycling receptors at the cell surface, and only apical proteins are internalized and delivered to the novel compartment.

The internalized apical proteins could have one of three possible fates: delivery to and degradation in lysosomes, retention at the compartment, or recycling to the PM. To discriminate among these possibilities, we examined the dynamics of apical proteins staged at the intracellular compartment. APN was surface labeled and chased to the compartment as described above (Figure 5a). The remaining PM-associated antibodies were stripped with isoglycine and only the internalized antibody–antigen complexes were protected and thus, detected (Figure 5c). After an additional hour at 37°C, APN was detected at the PM (Figure 5e).

Figure 4. The intracellular compartment receives apical proteins internalized from the PM, but not basolateral proteins or Tf-R. (A) Apical or basolateral proteins present at the cell surface were antibody labeled for 15 min at 4°C (a–d). Cells were incubated at 37°C for the indicated times, fixed, permeabilized, and labeled with Alexa-conjugated secondary antibodies to detect the trafficked antibody–antigen complexes. APN trafficked for 0 and 60 min in Fao cells (a and b), DPP IV trafficked for 90 min in Clone 9 cells (c), and HA321 trafficked for 60 min in Fao cells (d) are shown. DPP IV in Clone 9 cells was exogenously expressed with recombinant adenovirus. (B) In e and f, Fao cells were labeled with anti-APN antibodies at 4°C for 15 min. The antibody–antigen complexes were chased for 60 min at 37°C and the cells fixed and permeabilized. Both the trafficked (tr) anti-APN and steady-state (ss) anti-5'NT were detected with fluorescently conjugated secondary antibodies. Arrows are pointing to structures containing both APN and 5'NT. In h–j, PM-associated APN and Tf-R were colabeled for 15 min at 4°C in Fao cells and the antibody–antigen complexes chased at 37°C for 60 min. The arrows are pointing to structures containing only trafficked APN. Merged images are shown in g and j. Ap, apical; BL, basolateral. Bar, 10 µm.

Staining of nonpermeabilized cells processed in parallel (Figure 5, b, d, and f) verified these observations. Similar results were observed for DPP IV and 5'NT in Fao cells and DPP IV in Clone 9 cells (our unpublished data). These data indicate that the internalized apical proteins recycle to the PM.

### Apical Proteins Rapidly Recycle in Nonpolarized Cells

We also examined the internalization and recycling kinetics of apical proteins relative to the well-characterized Tf-R in Fao cells. As shown in Figure 6A, Tf-R was internalized with a $t_{1/2}$ of 2 min (rate = 10.8% of total internalized/min) reaching steady-state distributions after 30 min with $21.8 \pm 8.2\%$ at the PM. APN was also internalized rapidly with a $t_{1/2}$ of 5 min (rate = 6.4% of total internalized/min), and as for Tf-R, steady-state distributions were achieved after 30 min. But in this case, $68.5 \pm 7.8\%$ of APN was present at the PM. These reciprocal steady-state distributions are apparent in Figures 3, j–l, and 4, h–j. Similar kinetics and distributions were observed for DPP IV (our unpublished data).

To examine recycling kinetics, cells were continuously labeled with biotinylated anti-APN or anti-Tf-R antibodies for 2 h at 37°C. The remaining surface-associated antibodies were stripped and recycling of the intracellular pools to the PM was measured. Both Tf-R and APN rapidly recycled back to the PM with $t_{1/2}$ values of ~4 min, corresponding to rates of 2.1 and 7.6% of total Tf-R and APN recycled per minute, respectively (Figure 6B). Tf-R more rapidly reached its steady-state distributions (30 min) than APN (60 min). DPP IV's recycling kinetics were similar to that of APN (our unpublished data). Thus, the rate-limiting step in Tf-R's itinerary is recycling to the PM, whereas internalization is rate limiting for apical proteins.

Resident Apical Proteins Are Retained at Apical PM in Polarized Cells

We next asked whether resident apical proteins in polarized cells were dynamic. For these experiments, we monitored
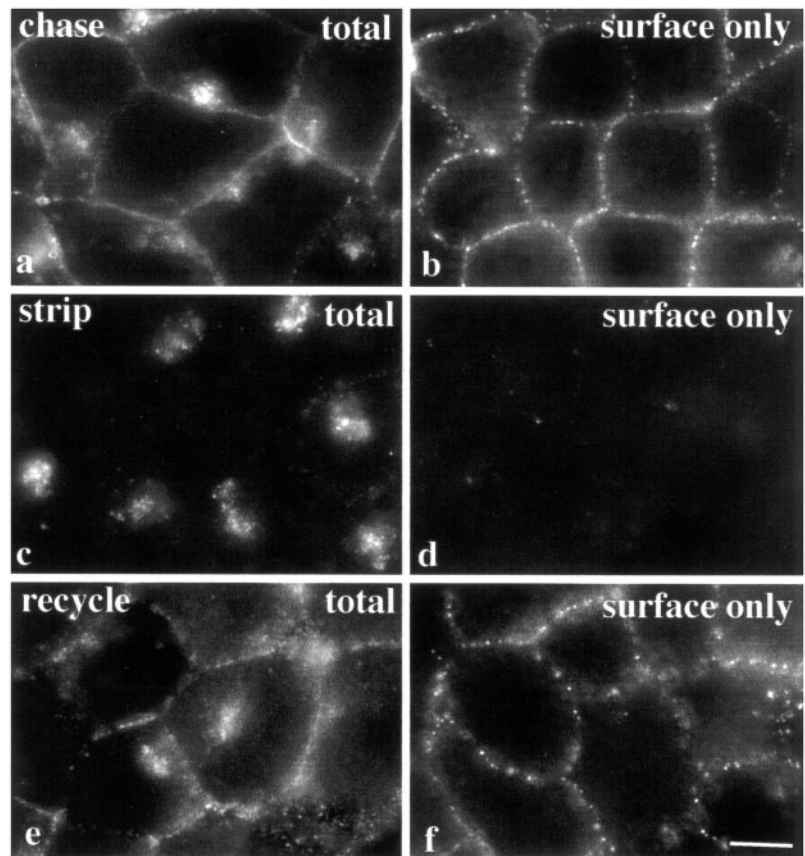
Figure 5. Apical proteins recycle between the intracellular compartment and the PM. Surface APN was antibody labeled and the antibody–antigen complexes chased for 1 h at 37°C in Fao cells (a and b). The remaining PM-associated antibodies were stripped with isoglycine for 5 min at RT (c and d). Only the protected, internalized APN–antibody complexes were detected (c). Cells were incubated an additional hour at 37°C (e and f). To detect the entire population of trafficked antibodies, cells were fixed and permeabilized (a, c, and e). To detect only the antigens present at the cell surface, cells were fixed in 4% PFA for 30 min at RT (b, d, and f). Bar, 10 μm.

populations of apically staged, antibody-labeled proteins in polarized WIF-B cells. APN present at the basolateral PM was continuously labeled for 1 h at 37°C and after washing, the complexes were chased for another hour. Although most of the labeled APN was chased to the apical PM, residual staining at the basolateral PM was observed (Figure 7, a and d), necessitating the use of isoglycine to remove this population (Figure 7, b and f). It is important to note that 10–20% of mature WIF-B cells are nonpolarized (Figure 7c). Interestingly, APN trafficked to intracellular structures in these nonpolarized WIF-B cells (Figure 7e) and isoglycine stripped anti-APN from the PM (Figure 7g). After stripping, all cells in the culture were incubated an additional hour at 37°C. Only APN in nonpolarized WIF-B cells recycled to the PM (Figure 7, c, i, and j). In polarized cells, APN staining was restricted to the apical PM (Figure 7, c, h, and j). At higher magnification, we observed that neither the basolateral PM nor any intracellular structures were labeled after the additional chase (Figure 7, h and j). Similar results were observed for 5′NT and pIgA-R (our unpublished data).

When we quantitated these observations (Figure 6C), we found that most of the polarized (~70%) and nonpolarized WIF-B cells (~90%) stained for APN at the basolateral PM and PM, respectively, after the initial uptake/chase period. After surface stripping, much of this staining was lost. However, after the additional incubation at 37°C, most of the nonpolarized cells regained their PM staining (~75%), whereas only ~20% of polarized cells were positive for

basolateral PM staining (Figure 6C, recycled bars). This last value is an over estimation of basolateral redistribution because >10% of the polarized cells were not efficiently surface stripped (Figure 6C, stripped bars). Thus, our results indicate that apical proteins are retained at the WIF-B apical PM but recycle in nonpolarized WIF-B cells.

Actin Regulates Apical Protein Dynamics in Polarized and Nonpolarized Cells

To characterize the mechanisms regulating apical protein dynamics in polarized and nonpolarized cells, we examined the effects of cytoskeletal disruption. In the presence of 33 μM nocodazole for 30 min, the MT network was completely disrupted in Fao cells (assayed by β-tubulin staining; our unpublished data) and the perinuclear location of the compartment was no longer apparent (compare Figure 8, a and b). However, small puncta in the cell periphery indicated that MT disruption had dispersed the compartment. When MTs were depolymerized before internalization of APN–antibody complexes, only small peripheral puncta were observed (our unpublished data). Interestingly, recycling was not inhibited by nocodazole, because surface labeling of APN staged at the intracellular compartment (see Figure 5c) was regained in both control (Figure 8c) and treated (Figure 8d) cells after the additional chase. Only peripheral APN-positive structures were observed in nocodazole-treated cells, further indicating that the organization of the compart-
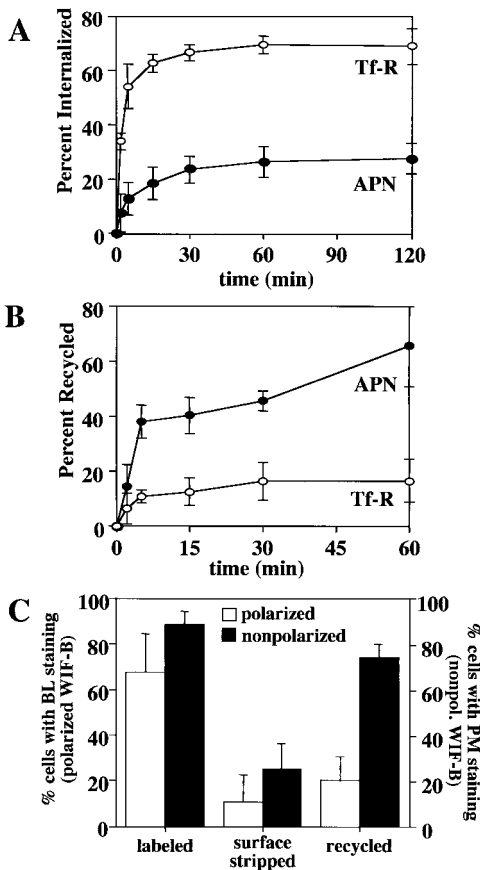
Figure 6. Apical proteins rapidly recycle in nonpolarized cells but are retained at the apical PM in polarized cells. (A) To measure internalization, Fao cells were continuously labeled with biotinylated antibodies for the indicated times at 37°C. The remaining PM-associated antibodies were eluted as described in Figure 5 and the cells lysed. Aliquots of the eluate and lysate (the internalized population) were assayed for amounts of biotinylated antibodies by using streptavidin-coated 96-well plates and colorimetric detection of HRP-conjugated secondary antibodies. Values are expressed as the mean ± SD. Measurements were done on at least three experiments each performed in duplicate. (B) To measure recycling, Fao cells were continuously labeled with biotinylated antibodies for 2 h at 37°C, eluted as described above, and returned to complete medium at 37°C for the indicated times. Cells were eluted again (the recycled population) and then lysed. The eluates and lysates were processed as for the internalization assays. Values are expressed as the mean ± SD. Measurements were done on at least three experiments each performed in duplicate. (C) APN at the basolateral PM of polarized WIF-B cells or at the PM of nonpolarized WIF-B cells was continuously labeled with specific antibodies for 1 h, the cells washed, and the antibody–antigen complexes chased for an additional hour (labeled). PM-associated antibodies were stripped with isoglycine for 2 min at 37°C (stripped). Cells were incubated an additional hour at 37°C (recycled). Random fields were visualized and cells scored for the presence of APN at the basolateral PM in polarized cells or at the PM in nonpolarized cells. Approximately 100–200 cells were counted for each condition. Values are expressed as the mean ± SD. Measurements were performed on four experiments.

ment is MT dependent. 5′NT and MRP2 behaved similarly (our unpublished data). We also monitored the distributions of apically staged APN in the presence of nocodazole and found that APN remained at the apical PM (Figure 8, f and

g). No intracellular accumulations were observed, further suggesting the proteins were apically retained and prevented from internalization. However, in treated nonpolarized WIF-B cells, APN recycled to the PM and the compartment was dispersed (Figure 8g).

Actin depolymerization also altered the compartment's morphology in Fao cells, but differently than nocodazole. Treatment with 1 μM CD for 30 min led to increased numbers of APN-positive intracellular structures (compare Figure 9, a and b). When we examined the dynamics of APN–antibody complexes in CD-treated cells, we observed uptake (our unpublished data), but little to no recycling to the PM (compare Figure 9, c and d). 5′NT and MRP2 behaved similarly (our unpublished data).

We also monitored the distributions of apical residents in the presence of 10 μM CD in polarized WIF-B cells. This higher concentration was required to disrupt the dense actin web surrounding the apical PM. Actin disassembly was monitored by Texas Red-phalloidin staining (our unpublished data) but was also apparent by the altered morphology of some of the apical surfaces (Figure 9, f and g). In nonpolarized WIF-B cells, apical protein recycling was impaired by actin disruption as observed in Fao cells (Figure 9f, asterisks). However, in treated polarized cells, single TMD and GPI-anchored apical residents redistributed to the basolateral PM after the additional chase (Figure 9, f and h). Quantitation showed only 15% of untreated polarized WIF-B cells were positive for basolateral staining, whereas nearly 65% of treated cells were positive. Similar results were obtained for pIgA-R (our unpublished data). Surprisingly, CD did not alter MRP2 distributions (Figure 9, g and h). In both control and treated polarized cells, <2% of cells were positive for basolateral MRP2 staining (Figure 9, g and h).

To rule out that CD was disrupting tight junction function, we measured the permeability properties of BCs to FITC-conjugated dextran (71.2 kDa) as described previously (Ihrke *et al.*, 1993). Approximately 75% of BCs were impermeable to the dextran in both control and treated cells. These results indicate that tight junction integrity was not impaired by CD treatment, thus lateral diffusion does not explain the appearance of certain classes of apical residents at the basolateral PM. Rather, we conclude that actin-dependent retention mechanisms selectively operate at the apical PM in polarized WIF-B cells.

DISCUSSION

We found that apical proteins are present in two pools in nonpolarized cells: at the PM and in an intracellular compartment that contains only other apical proteins. No coincident intracellular staining patterns were observed between apical proteins and markers of the biosynthetic or endocytic pathways. We also determined that the compartment is dynamic (apical proteins recycle between it and the PM) and selective (basolateral proteins and recycling receptors are excluded). Thus, polarized sorting from the PM occurs in nonpolarized cells as in polarized cells. Importantly, we discovered one major difference in apical protein dynamics between the two cell types. Nonpolarized cells require intact actin filaments to recycle apical proteins from the intracellular compartment, whereas polarized cells require intact actin filaments to retain the same proteins at the apical
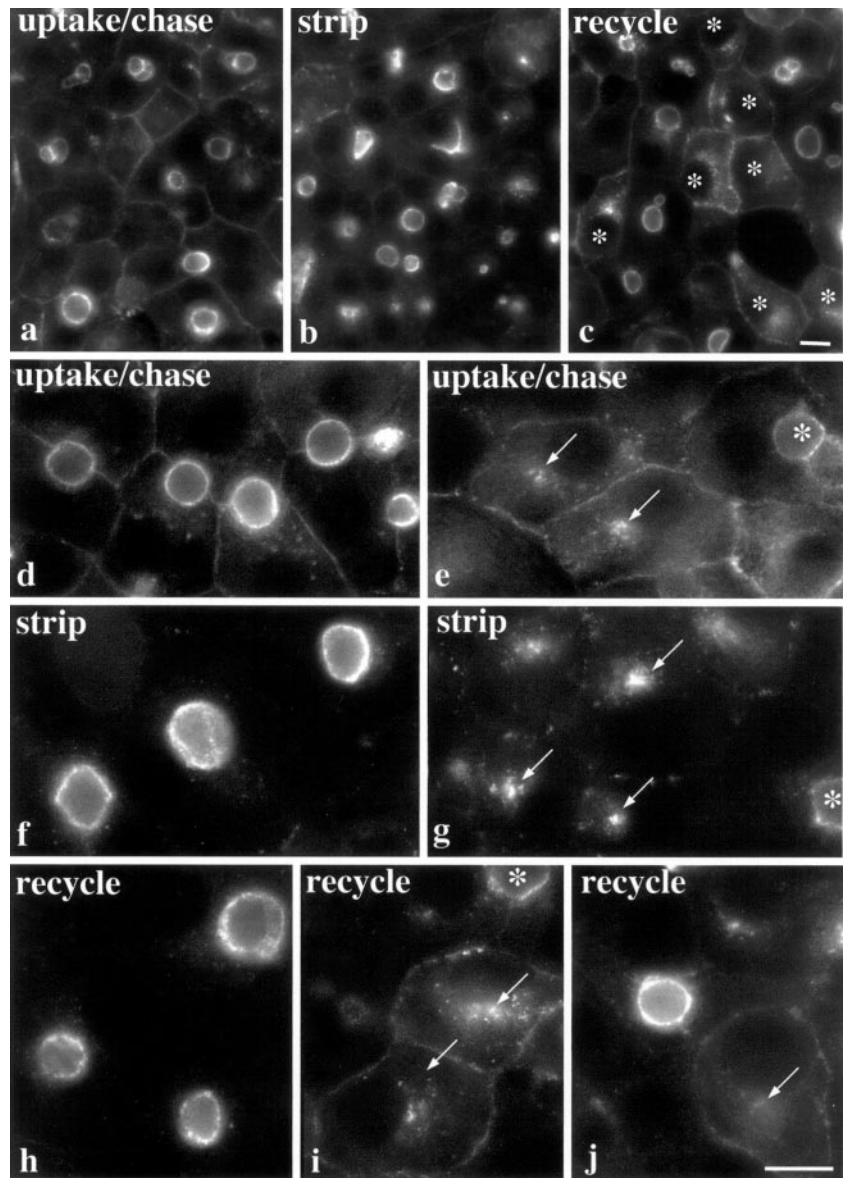
Figure 7. Apical proteins are retained at the apical PM in polarized WIF-B cells. APN at the basolateral PM was continuously labeled with specific antibodies for 1 h, the cells washed, and the antibody–antigen complexes chased to the apical PM for an additional hour. A low-magnification image (a) shows both polarized and nonpolarized WIF-B cells. Higher magnification images of labeled polarized (d) and nonpolarized (e) WIF-B cells are also shown. APN antibodies remaining at the basolateral PM were stripped with isoglycine for 2 min at 37°C. Only the APN–antibody complexes present at the apical PM in polarized cells or in the intracellular compartment in nonpolarized WIF-B cells were detected (b). Higher magnification images of stripped polarized (f) and nonpolarized (g) WIF-B cells are also shown. Cells shown in c, h, i, and j were incubated an additional hour at 37°C after stripping. Only apical proteins in the nonpolarized cells recycled to the PM as indicated with asterisks (c). Higher magnification images of polarized cells (h and j) further show that no intracellular populations of APN were observed after the additional chase, whereas in nonpolarized WIF-B cells (i and j) recycling was evident. Arrows point to the labeled compartment in nonpolarized cells and the asterisk in i points to an apical surface in a polarized cell. Bar, 10 μm.

surface. This difference suggests a possible role for actin-based mechanisms in regulating apical polarity in hepatic cells.

Domain-Specific Protein Trafficking in Polarized and Nonpolarized Cells

The trafficking of apical proteins in polarized and nonpolarized hepatic cells is summarized in Figure 10. In polarized cells, newly synthesized apical and basolateral proteins are sorted from the TGN to the basolateral PM. The apical proteins are selectively internalized from the basolateral PM and transcytosed to the apical surface (Bartles *et al.*, 1987; Bartles and Hubbard, 1988; Schell *et al.*, 1992, Ihrke *et al.*, 1998) where they are retained until signaled for lysosomal delivery (Tuma *et al.*, 1999, 2001). In nonpolarized cells,

apical and basolateral proteins are also delivered to the PM from the TGN. We do not know whether the proteins are sorted into separate vesicles, but results from other nonpolarized cells suggest that they are (Musch *et al.*, 1996; Yoshimori *et al.*, 1996). As in polarized cells, the apical proteins are selectively internalized from the PM and delivered to structures containing only other apical proteins ("apical" compartment). The novelty of the apical organelle further suggests it is formed by homotypic fusion of vesicles containing apical proteins. In the absence of retention mechanisms in this compartment, the apical proteins recycle to the PM.

In nonpolarized Fao and WIF-B cells, both the compartment's location and dependence on MTs for organization suggest it is located at the MT organizing center (MTOC). Double labeling with γ-tubulin, an MTOC resident, was
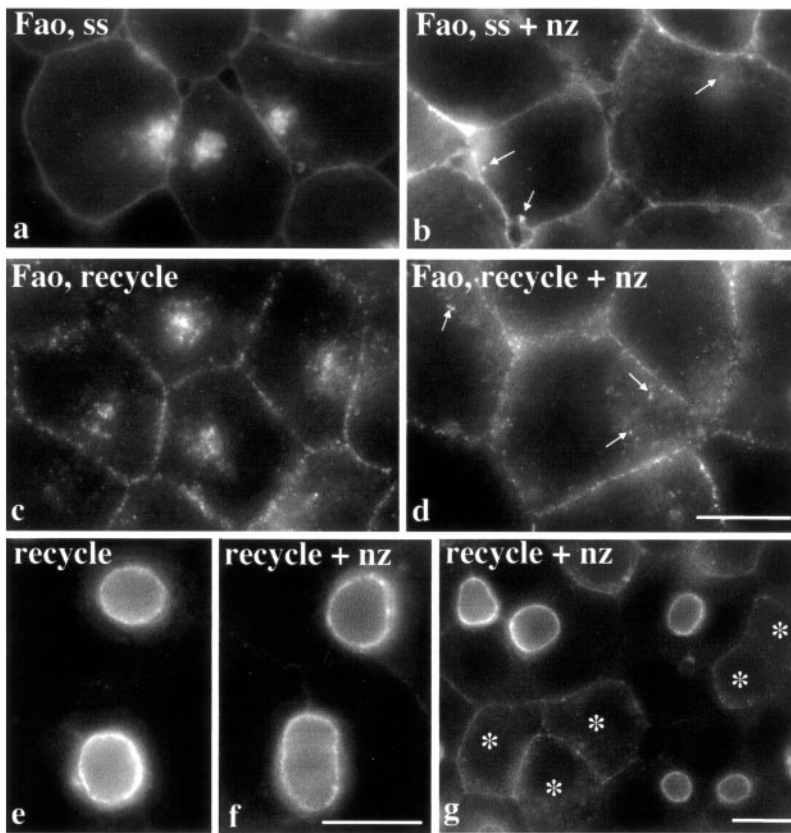
Figure 8. Organization of the intracellular compartment in nonpolarized cells is MT dependent. Steady-state (ss) distributions of APN were examined after incubation of Fao cells in the absence (a) or presence (b) of 33 μM nocodazole (nz) for 30 min at 37°C. Arrows in b point to the dispersed compartment. In c and d, cell surface APN was antibody-labeled for 15 min at 4°C and the antibody–antigen complexes chased for 1 h at 37°C in Fao cells. The remaining surface anti-APN was stripped with isoglycine for 5 min at RT. Cells were incubated an additional hour at 37°C in the absence (c) or presence (d) of 33 μM nocodazole. Arrows in d are pointing to small, APN-positive puncta in the cell periphery. The recycling assay was performed in WIF-B cells as described in Figure 7 in the absence (e) or presence (f and g) of 33 μM nocodazole. Recycling was observed only in nonpolarized WIF-B cells as indicated with asterisks. Bar, 10 μm.

consistent with this conclusion (our unpublished data). In comparison, MT minus ends terminate at the apical PM in polarized WIF-B cells (Meads and Schroer, 1995). Thus, in both polarized and nonpolarized cells, the internalized apical proteins are delivered to compartments situated at MT minus ends.

This model raises many interesting possibilities. First, nonpolarized cells are equipped with the proper machinery to specifically internalize apical residents from the PM and deliver them to a discrete cellular location (apical compartment vs. apical PM). We suggest this represents the transcytotic pathway because basolateral residents and recycling receptors are excluded. Also, the apical protein half-lives are 1–2 d in both WIF-B and Fao cells (our unpublished data), indicating that apical proteins are not prematurely degraded in nonpolarized cells. This further implies that the signals mediating lysosome delivery and degradation are present in nonpolarized cells and that retention does not stabilize the apical residents in WIF-B cells. The major difference in apical protein itineraries in the two cell types is differing retention at their specific subcellular locations.

Although it is clear that mature apical residents are less dynamic in polarized cells than in nonpolarized cells, we cannot exclude the possibility that local apical PM recycling is occurring, but is below the resolution of light microscopic detection. However, when we monitored apically staged APN–antibody complexes for longer incubations (3 h), we could detect intracellular APN (our unpublished data). Because this labeling was enhanced by leupeptin treatment, we

suggest it represents the population of APN destined for degradation (Tuma *et al.*, 2001). Because only ~2–3% of APN is estimated to be degraded per hour, the morphological methods we used detected small amounts of protein. Thus, if local apical recycling is occurring in WIF-B cells, the levels must be very low.

Is the Apical Compartment the Subapical Compartment (SAC) or a Pseudoapical Domain?

At present, we cannot discriminate whether the apical compartment described herein is a pseudoapical domain or the SAC, the final intermediate of the transcytotic pathway identified in intact hepatocytes and polarized WIF-B cells (Barr *et al.*, 1993; Ihrke *et al.*, 1998). Presently, no markers have been identified that specifically label the SAC at steady state, precluding the definitive identification of the apical compartment described herein. Although in nonpolarized cells, rab11a labels recycling endosomes, in polarized cells, it stains apical recycling endosomes, possible analogous structures to the hepatic SAC (Wang *et al.*, 2000). Thus, the absence of rab11a staining in the apical compartment argues it is not the SAC.

By examining the dynamics of the short chain fluorescent lipid analogs 6-[*N*-(7-nitrobenz-2-oxa-1,3 diazol-4-yl)amino]hexanoic acid (C$_6$NBD)-sphingomyelin and C$_6$NBD-glucosyl-ceramide in HepG2 cells, Hoekstra and colleagues have identified a compartment that has also been named the SAC (reviewed in van IJzendoorn and Hoekstra, 1999). More
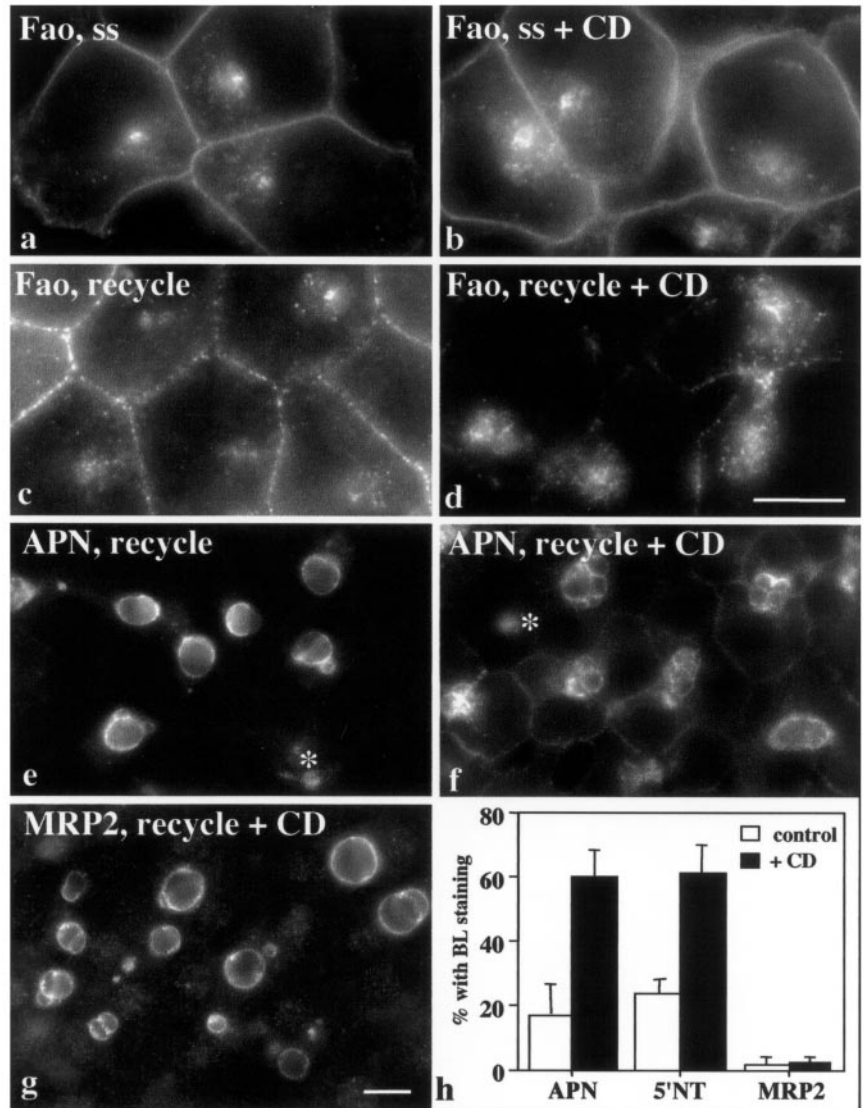
Figure 9. Recycling in nonpolarized cells and retention of single TMD and GPI-anchored proteins in polarized cells are actin dependent. Steady-state (ss) distributions of APN were examined in Fao cells treated in the absence (a) or presence (b) of 1 μM CD for 30 min at 37°C. In c and d, surface APN was antibody labeled for 1 h at 37°C in Fao cells. The remaining surface anti-APN was stripped with isoglycine for 5 min at RT, and the cells were incubated an additional hour at 37°C in the absence (c) or presence (d) of 1 μM CD. Bar, 10 μm. Apical PM dynamics were measured in WIF-B cells in the absence or presence of 10 μM CD (e–h). For APN and 5'NT, dynamics were assayed as described in Figure 6. Because no basolateral populations of MRP2 are detected, steady-state MRP2 distributions were determined in the absence or presence (f) of 10 μM CD for 1 h at 37°C. Asterisks in f are marking nonpolarized WIF-B cells where recycling of apical proteins was impaired. In treated polarized cells, APN (f and h) and 5'NT (h) redistributed to the basolateral PM, whereas MRP2 (g and h) distributions did not change. Bar, 10 μm. In h, random fields of control or CD-treated polarized WIF-B cells were scored for the presence of the indicated apical proteins at the basolateral PM. Cells (100–200) were counted for each condition per experiment. Values are expressed as the mean $\pm$ SD. Measurements were performed on at least three experiments.

recently they determined that this compartment changes during the development of surface polarity (van IJzendoorn and Hoekstra, 2000). Although it is not clear whether this SAC is the same as the one described above, important differences between lipid and protein trafficking have been described. The basolateral-to-apical transport of both lipids and proteins is vesicle mediated, but unlike for transcytosing proteins, the SAC seems not to be an intermediate in the lipid transport pathway because NBD puncta are present elsewhere in the cell. However, in Hep-G2 cells overexpressing pIgA-R, a partial overlap between transcytosing IgA ligand (presumed to be in SAC) and NBD-sphingolipids derived from the apical PM after an 18°C temperature block was observed (van IJzendoorn and Hoekstra, 1998). These data suggest that the lipids recycled to the SAC. To date, recycling of proteins from the apical PM to the SAC has not been observed in intact hepatocytes or WIF-B cells (Barr *et al.*, 1993, Ihrke *et al.*, 1998; reviewed in Tuma and Hubbard,

2001). Curiously, basolateral-to-apical transcytosis of the lipids was not inhibited by microtubule disruption, although their internalization at the basolateral PM was decreased by actin depolymerization. In contrast, we find that transcytosis of apical PM proteins transiently present in the basolateral PM of WIF-B cells is significantly inhibited by microtubule disruption and unaffected by actin depolymerization. Thus, important differences exist between the trafficking of apical PM proteins and C$_6$-NBD-lipids. Until specific steady state SAC markers are identified we cannot definitively identify whether the "lipid" and "protein" SACs are the same or whether the apical compartment described in this study represents either (or both) of these intermediates.

Apical Compartment Is Novel

The apical compartment identified in this study is not the vacuolar apical compartment (VAC) that was previously

Polarized Hepatic Cells

Nonpolarized Hepatic Cells
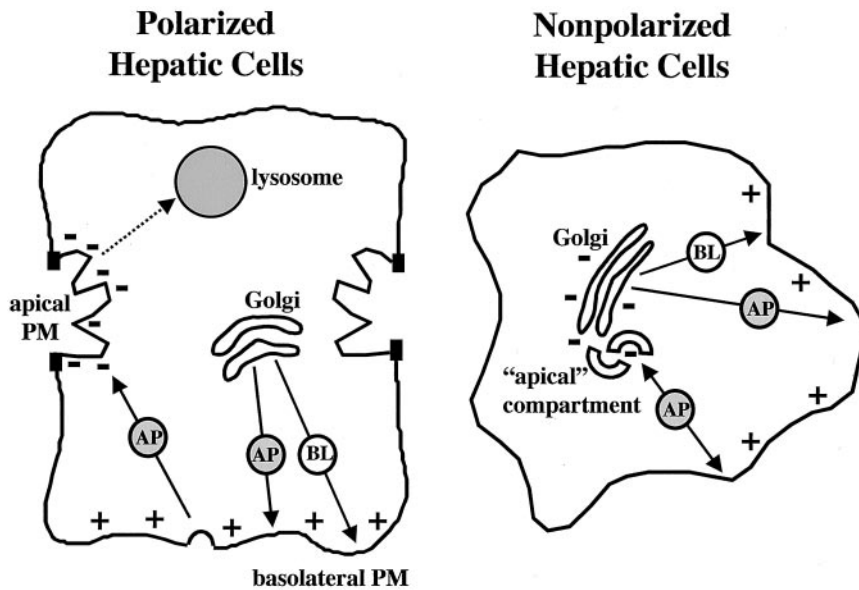
Figure 10. Intracellular itineraries of apical proteins in polarized and nonpolarized hepatic cells. In polarized cells, newly synthesized apical proteins are delivered from the TGN to the basolateral PM. They are selectively retrieved by endocytosis and transcytosed to the apical PM. Apical proteins are retained at the apical PM until signaled for lysosomal delivery and degradation. In nonpolarized cells, apical proteins are delivered from the TGN to the PM and are selectively internalized and transported to a novel apical compartment. The proteins rapidly recycle between this compartment and the PM. MT polarity ($-$, minus ends; $+$, plus ends) is also indicated. AP, apical; BL, basolateral.

identified in nonpolarized epithelial cells (Vega-Salas *et al.*, 1987, 1988; Gilbert and Rodriguez-Boulan, 1991; Low *et al.*, 2000). The apical structures we have described occur in normally growing cells that do not polarize (Fao and Clone 9) or in WIF-B cells that before they become polarized. The VAC was first identified in MDCK cells that were seeded at low density and grown in low Ca^{2+}, conditions that maintain single-cell colonies or prevent monolayers from forming cell-cell contacts (Vega-Salas *et al.*, 1987). VACs have also been described in Caco2 cells that were treated with nocodazole and colchicine for long periods, and their formation required new protein synthesis (Gilbert and Rodriguez-Boulan, 1991); the compartment described herein shares neither of these features. Furthermore, the compartments are morphologically distinct. Unlike the apical compartment we have described, VACs are large (0.5–5 μm), contain microvilli, and are not situated at the MTOC (Vega-Salas *et al.*, 1987). Similarly, the apical compartment is not the microvilli-lined vesicles (MLVs) identified previously in HepG2 cells (Zaal *et al.*, 1994). Like VACs, MLVs are large structures that contain microvilli and stain for actin, characteristics not shared by the apical compartment we described. From this comparison, it is clear that the compartment described herein is neither a VAC nor an MLV and may represent a more physiologically relevant intermediate in nonpolarized cells.

Recently, an endosomal compartment was identified as an intermediate in PM-to-Golgi trafficking (Nichols, 2002). Like our compartment, this endosome received GPI-anchored proteins while it excluded "classical" endosomal markers such as EEA1, rab5, transferring, and rab11. However, in the nonpolarized hepatic cells, the apical compartment is the destination of the GPI-anchored apical proteins rather than an intermediate en route to the Golgi. Furthermore, the PM-to-TGN endosomes were positive for caveolin-1, a protein not expressed (or at extremely low levels) in hepatic cells (our unpublished data). Also fluid phase markers labeled the caveolin-positive compartment, whereas they are excluded from the apical compartment. Together, these data suggest that these are distinct endosomal populations.

Retention vs. Recycling

The paradox presented in this study is the differential requirement for actin in recycling and retention in polarized and nonpolarized cells. Nonpolarized recycling is impaired when actin is depolymerized, thus retention is enhanced. Conversely, in polarized cells retention mechanisms are impaired by CD and enhanced recycling was observed. What explains these differential effects?

The examination of Tf dynamics in nonpolarized or polarized cells has revealed that PM recycling is actin dependent (Durrbach *et al.*, 1996b, 2000; reviewed in Apodaca, 2001). Characterization of myosin motors, likely candidates for mediating actin-based vesicle motility, has also suggested that actin regulates recycling (reviewed in Baker and Titus, 1998; Mermall *et al.*, 1998). For example, overexpression of dominant negative myosin 1 dispersed a Tf-positive compartment in hepatoma cells (Durrbach *et al.*, 1996a) and significantly decreased basolateral Tf recycling in Caco2 cells (Durrbach *et al.*, 2000). The expression of mutant Cdc42, an actin-modifying GTPase, also led to decreased Tf recycling in MDCK cells (Kroschewski *et al.*, 1999). Because myosin motors have been localized to different endosomal populations, they may mediate transport at multiple steps (Raposo *et al.*, 1999; Huber *et al.*, 2000; Lionne *et al.*, 2001). Thus, in nonpolarized cells, the actin dependence of apical protein recycling may be explained by a requirement for myosin motors or actin-associated GTPases.

In polarized cells, actin is generally considered an important regulator of apical, but not basolateral, endocytosis. Addition of CD impaired internalization of multiple markers only from the apical domain in MDCK, Caco2, and pancreatic acinar cells (Gottlieb *et al.*, 1993; Jackman *et al.*, 1994; Shurety *et al.*, 1996; Valentijn *et al.*, 1999). Ultrastructural and biochemical analysis further suggested that clath-

rin- and nonclathrin-mediated internalization mechanisms were impaired. Unfortunately, apical PM proteins were not examined in these studies. However, our observations that CD led to the basolateral distribution of certain apical proteins (implying increased apical endocytosis) are not consistent with these results. This may be explained in part by the emerging hypothesis that domain-specific proteins maintain their polarized distributions by actin-based scaffolds that actively exclude them from endocytosis (reviewed in Yeaman *et al.*, 1999). In particular, the ezrin-radixin-moesin (ERM) proteins have been identified as mediators of actin-membrane attachment (reviewed in Mangeat *et al.*, 1999, Bretscher *et al.*, 2000). Because ERM proteins can bind both single-spanning apical proteins and actin directly, they have also been implicated as regulators of apical retention; ERM proteins cross-link apical residents to the underlying cortical web tethering them into place. We do not know whether the apical proteins we examined bind ERM proteins directly, but interactions with GPI-anchored proteins must be indirect and mediated by other TMD proteins. Although such proteins have not been identified, biophysical evidence for such interactions has been described previously (Suzuki and Sheetz, 2001).

Polytopic PM residents also interact with ERM proteins, but these associations are mediated by PDZ proteins (reviewed in Fanning and Anderson, 1999). One such PDZ protein, EBP50 (also called NHERF; Shenolikar and Weinman, 2001), binds both polytopic apical proteins and ERM proteins. E3KARP, another apical PDZ protein, has also been shown to bind ezrin (Yun *et al.*, 1997). Thus, these and other PDZ proteins are thought to form large scaffolds that tether polytopic apical residents to the actin web. MRP2 encodes a PDZ binding domain that can bind PDZK1, another PDZ protein, in vitro (Kocher *et al.*, 1999). However, PDZK1 is present at the basolateral PM in hepatic cells (our unpublished data), suggesting other PDZ proteins (EBP50 or E3KARP?) are mediating MRP2 apical actin association. Neither MRP2 nor EBP50 distributions were altered in CD-treated cells, whereas radixin and ezrin apical distributions were partially disrupted (our unpublished data). Thus, unlike ERM interactions with single TMD proteins in CD-treated cells, PDZ proteins may not dissociate from polytopic proteins maintaining apical retention.

Apical Compartment Is an Intermediate in Apical PM Formation

Earlier work suggested that nonpolarized cells are capable of polarized PM delivery, but lack the spatial segregation of distinct membrane targets. Our work extends that conclusion and demonstrates that nonpolarized cells also sort proteins at the PM and deliver them to specific subcellular locations. In particular, apical proteins are delivered to novel structures that we propose are intermediates in apical PM formation. In the absence of retention mechanisms, apical proteins recycle apparently randomly to the nondifferentiated PM. Upon appropriate extrinsic signals, asymmetric PM cues are established that may lead to local actin reorganization and the formation of "targeting patches" that receive specific membrane cargo (reviewed in Yeaman *et al.*, 1999). As the PM segregates, the apical vesicles are readily targeted to specific domains and establish an apical patch that eventually forms the apical surface. Although Fao or

Clone 9 cells do not polarize, the apical compartment is present suggesting that key molecular players may be differentially expressed such that polarity is not achieved. Alternatively, the compartment's presence in nonpolarized cells may indicate that all cells are equipped for the rapid response to extrinsic cues that set up a spatially segregated PM, which promotes directed cell motility, cell shape changes, or targeted endocytosis or exocytosis.

REFERENCES

Apodaca, G. (2001). Endocytic traffic in polarized epithelial cells: role of the actin and microtubule cytoskeleton. Traffic 2, 149–159.

Baker, J.P., and Titus, M.A. (1998). Myosins: matching functions with motors. Curr. Opin. Cell Biol. 10, 80–86.

Barr, V.A., and Hubbard, A.L. (1993). Newly synthesized hepatocyte plasma membrane proteins are transported in transcytotic vesicles in the bile duct-ligated rat. Gastroenterology 105, 554–571.

Bartles, J.R., Feracci, H.M., Stieger, B., and Hubbard, A.L. (1987). Biogenesis of the rat hepatocyte plasma membrane in vivo: comparison of the pathways taken by apical and basolateral proteins using subcellular fractionation. J. Cell Biol. 105, 1241–1251.

Bartles, J.R., and Hubbard, A.L. (1986). Preservation of hepatocyte plasma membrane domains during cell division in situ in regenerating rat liver. Dev. Biol. 118, 286–295.

Bartles, J.R., and Hubbard, A.L. (1988). Plasma membrane protein sorting in epithelial cells: do secretory pathways hold the key? Trends Biochem. Sci. 13, 181–184.

Bastaki, M., Braiterman, L.T., Johns, D.C., Chen, Y.-H., and Hubbard, A.L. (2002). Absence of direct delivery for single transmembrane apical proteins or their "secretory" forms in polarized hepatic cells. Mol. Biol. Cell 13, 225–237.

Bretscher, A., Chambers, D., Nguyen, R., and Reczek, D. (2000). ERM-Merlin and EBP50 protein families in plasma membrane organization and function. Annu. Rev. Cell Dev. Biol. 16, 113–143.

Durrbach, A., Collins, K., Matsudaira, P., Louvard, D., and Coudrier, E. (1996a). Brush border myosin I truncated in the motor domain impairs the distribution and the function of endocytic compartments in an hepatoma cell line. Proc. Natl. Acad. Sci. USA 93, 7053–7058.

Durrbach, A., Louvard, D., and Coudrier, E. (1996b). Actin filaments facilitate two steps of endocytosis. J. Cell Sci. 109, 457–465.

Durrbach, A., Raposo, G., Tenza, D., Louvard, D., and Coudrier, E. (2000). Truncated brush border myosin I affects membrane traffic in polarized epithelial cells. Traffic 1, 411–424.

Fanning, A.S., and Anderson, J.M. (1999). Protein modules as organizers of membrane structure. Curr. Opin. Cell Biol. 11, 432–439.

Feracci, H., Connolly, T.P., Margolis, R.N., and Hubbard, A.L. (1987). The establishment of hepatocyte cell surface polarity during fetal liver development. Dev. Biol. 123, 73–84.

Fiedler, K., Lafont, F., Parton, R.G., and Simons, K. (1995). Annexin XIIIb: a novel epithelial specific annexin is implicated in vesicular traffic to the apical plasma membrane. J. Cell Biol. *128*, 1043–1053.

Gilbert, T., and Rodriguez-Boulan, E. (1991). Induction of vacuolar apical compartments in the Caco-2 intestinal epithelial cell line. J. Cell Sci. *100*, 451–458.

Gottlieb, T.A., Ivanov, I.E., Adesnik, M., and Sabatini, D.A. (1993). Actin microfilaments play a critical role in endocytosis at the apical but not the basolateral surface of polarized epithelial cells. J. Cell Biol. *120*, 695–710.

Hubbard, A.L., Bartles, J.R., and Braiterman, L.T. (1985). Identification of rat hepatocyte plasma membrane proteins using monoclonal antibodies. J. Cell Biol. *100*, 1115–1125.

Huber, L.A., Fialka, I., Paiha, K., Hunziker, W., Sacks, D.B., Bahler, M., Way, M., Gagescu, R., and Gruenberg, J. (2000). Both calmodulin and the unconventional myosin Myr4 regulate membrane trafficking along the recycling pathway of MDCK cells. Traffic *1*, 494–503.

Ihrke, G., Martin, G.V., Shanks, M.R., Schrader, M., Schroer, T.A., and Hubbard, A.L. (1998). Apical plasma membrane proteins and endolyn-78 travel through a subapical compartment in polarized WIF-B hepatocytes. J. Cell Biol. *141*, 115–133.

Ihrke, G., Neufeld, E.B., Meads, T., Shanks, M.R., Cassio, D., Laurent, M., Schroer, T.A., Pagano, R.E., and Hubbard, A.L. (1993). WIF-B cells: an in vitro model for studies of hepatocyte polarity. J. Cell Biol. *123*, 1761–1775.

Jackman, M.R., Shurety, W., Ellis, J.A., and Luzio, J.P. (1994). Inhibition of apical but not basolateral endocytosis of ricin and folate in Caco-2 cells by cytochalasin D. J. Cell Sci. *107*, 2547–2556.

Kocher, O., Comella, N., Gillchrist, A., Pal, R., Tgnazzi, K., Brown, L.F., and Knoll, J.H. (1999). PDZK1, a novel PDZ domain-containing protein up-regulated in carcinomas and mapped to chromosome 1q21, interacts with cMOAT (MRP2), the multidrug resistance-associated protein. Lab. Invest. *79*, 1161–1170.

Kroschewski, R., Hall, A., and Mellman, I. (1999). Cdc42 controls secretory and endocytic transport to the basolateral plasma membrane of MDCK cells. Nat. Cell Biol. *1*, 8–13.

Larkin, J.M., Woo, B., Balan, V., Marks, D.L., Oswald, B.J., LaRusso, N.F., and McNiven, M.A. (2000). Rab3D, a small GTP-binding protein implicated in regulated secretion, is associated with the transcytotic pathway in rat hepatocytes. Hepatology *32*, 348–356.

Lionne, C., Buss, F., Hodge, T., Ihrke, G., and Kendrick-Jones, J. (2001). Localization of myosin Va is dependent on the cytoskeletal organization in the cell. Biochem. Cell Biol. *79*, 93–106.

Low, S.H., Miura, M., Roche, P.A., Valdez, A.C., Mostov, K.E., and Weimbs, T. (2000). Intracellular redirection of plasma membrane trafficking after loss of epithelial cell polarity. Mol. Biol. Cell *11*, 3045–3060.

Lutcke, A., Jansson, S., Parton, R.G., Chavrier, P., Valencia, A., Huber, L.A., Lehtonen, E., and Zerial, M. (1993). Rab17, a novel small GTPase, is specific for epithelial cells and is induced during cell polarization. J. Cell Biol. *121*, 553–564.

Mangeat, P., Roy, C., and Martin, M. (1999). ERM proteins in cell adhesion and membrane dynamics. Trends Cell Biol. *9*, 187–192.

Meads, T., and Schroer, T.A. (1995). Polarity and nucleation of microtubules in polarized epithelial cells. Cell Motil. Cytoskeleton *32*, 273–288.

Mermall, V., Post, P.L., and Mooseker, M.S. (1998). Unconventional myosins in cell movement, membrane traffic, and signal transduction. Science *279*, 527–533.

Musch, A., Xu, H., Shields, D., and Rodriguez-Boulan, E. (1996). Transport of vesicular stomatitis virus G protein to the cell surface is signal mediated in polarized and nonpolarized cells. J. Cell Biol. *133*, 543–558.

Nichols, B.J. (2002). A distinct class of endosome mediates clathrin-independent endocytosis to the Golgi complex. Nat. Cell Biol. *4*, 3744–378.

Raposo, G., Cordonnier, M.N., Tenza, D., Menichi, B., Durrbach, A., Louvard, D., and Coudrier, E. (1999). Association of myosin I α with endosomes and lysosomes in mammalian cells. Mol. Biol. Cell *10*, 1477–1494.

Schell, M.J., Maurice, M., Stieger, B., and Hubbard, A.L. (1992). 5′ Nucleotidase is sorted to the apical domain of hepatocytes via an indirect pathway. J. Cell Biol. *119*, 1173–1182.

Scott, L.J., and Hubbard, A.L. (1992). Dynamics of four rat liver plasma membrane proteins and polymeric IgA receptor. Rates of synthesis and selective loss into the bile. J. Biol. Chem. *267*, 6099–6106.

Shanks, M.S., Cassio, D., Lecoq, O., and Hubbard, A.L. (1994). An improved rat hepatoma hybrid cell line. Generation and comparison with its hepatoma relatives and hepatocytes in vivo. J. Cell Sci. *107*, 813–825.

Shenolikar, S., and Weinman, E.J. (2001). NHERF: targeting and trafficking membrane proteins. Am. J. Physiol. *280*, F389–F395.

Shurety, W., Bright, N.A., and Luzio, J.P. (1996). The effects of cytochalasin D and phorbol myristate acetate on the apical endocytosis of ricin in polarised Caco-2 cells. J. Cell Sci. *109*, 2927–2935.

Suzuki, K., and Sheetz, M.P. (2001). Binding of cross-linked glycosylphosphatidylinositol-anchored proteins to discrete actin-associated sites and cholesterol-dependent domains. Biophys. J. *81*, 2181–2189.

Tuma, P.L., Finnegan, C.M., Yi, J.H., and Hubbard, A.L. (1999). Evidence for apical endocytosis in polarized hepatic cells: phosphoinositide 3-kinase inhibitors lead to the lysosomal accumulation of resident apical plasma membrane proteins. J. Cell Biol. *145*, 1089–1102.

Tuma, P.L., and Hubbard, A.L. (2001). The hepatocyte surface: dynamic polarity. In: The Liver: Biology and Pathobiology, ed. I.M Arias, J.L Boyer, F.V. Chisari, N. Fausto, D. Schachter, and D.A. Shafritz, Philadelphia: Lippincott Williams & Wilkins, 98–117.

Tuma, P.L., Nyasae, L.K., Backer, J.M., and Hubbard, A.L. (2001). Vps34p differentially regulates endocytosis from the apical and basolateral domains in polarized hepatic cells. J. Cell Biol. *154*, 1197–1208.

Valentijn, K.M., Gumkowski, F.D., and Jamieson, J.D. (1999). The subapical actin cytoskeleton regulates secretion and membrane retrieval in pancreatic acinar cells. J. Cell Sci. *112*, 81–96.

van IJzendoorn, S.D.C., and Hoekstra, D. (1998). (Glyco)sphingolipids are sorted in sub-apical compartments in HepG2 cells: a role for non-Golgi-related intracellular sites in the polarized distribution of (glyco)sphingolipids. J. Cell Biol. *142*, 347–357.

van IJzendoorn, S.C.D., and Hoekstra, D. (1999). The subapical compartment: a novel sorting center? Trends Cell Biol. *9*, 144–149.

van IJzendoorn, S.C.D., and Hoekstra, D. (2000). Polarized sphingolipid transport from the subapical compartment changes during cell polarity development. Mol. Biol. Cell. *11*, 1093–1101.

Vega-Salas, D.E., Salas, P.J., and Rodriguez-Boulan, E. (1987). Modulation of the expression of an apical plasma membrane protein of Madin-Darby canine kidney epithelial cells: cell-cell interactions control the appearance of a novel intracellular storage compartment. J. Cell Biol. *104*, 1249–1259.

Vega-Salas, D.E., Salas, P.J.I., and Rodriguez-Boulan, E. (1988). Exocytosis of vacuolar apical compartment (VAC): a cell-cell contact

controlled mechanism for the establishment of the apical plasma membrane domain in epithelial cells. J. Cell Biol. *107*, 1717–1728.

Wandinger-Ness, A., Bennett, M.K., Antony, C., and Simons, K. (1990). Distinct transport vesicles mediate the delivery of plasma membrane proteins to the apical and basolateral domains of MDCK cells. J. Cell Biol. *111*, 987–1000.

Weinstein, I.B., Orenstein, J.M., Gebert, R., Kaighn, M.E., and Stadler, U.C. (1975). Growth and structural properties of epithelial cell cultures established from normal rat liver and chemically induced hepatomas. Cancer Res. *35*, 253–263.

Wang, X., Kumar, R., Navarre, J., Casanova, J.E., and Goldenring, J.R. (2000). Regulation of vesicle trafficking in MDCK cells by Rab11a and Rab25. J. Biol. Chem. *275*, 29138–29146.

Yeaman, C., Grindstaff, K.K., and Nelson, W.J. (1999). New perspectives on mechanisms involved in generating epithelial cell polarity. Physiol. Rev. *79*, 73–98.

Yoshimori, T., Keller, P., Roth, M.G., and Simons, K. (1996). Different biosynthetic transport routes to the plasma membrane in BHK and CHO cells. J. Cell Biol. *133*, 247–256.

Yun, C.H., Oh, S., Zizak, M., Steplock, D., Tsao, S., Tse, C.M., Weinman, E.J., and Donowitz, M. (1997). cAMP-mediated inhibition of the epithelial brush border Na^+/H^+ exchanger, Nhe3, requires an associated regulatory protein. Proc. Natl. Acad. Sci. USA *94*, 3010–3015.

Zaal, K.J.M., Kok, J.W., Sormunen, R., Eskelinen, S., and Hoekstra, D. (1994). Intracellular sites involved in the biogenesis of bile canaliculi in hepatic cells. Eur. J. Cell Biol. *63*, 10–19.